Agricultural and Forest Meteorology, 61 (1992) 23–38
Elsevier Science Publishers B.V., Amsterdam

Simulation of soil temperature in crops

Y. Luo[a], R.S. Loomis[a] and T.C. Hsiao[b]

[a]*Department of Agronomy and Range Science, University of California, Davis, CA 95616, USA*
[b]*Department of Land, Air, and Water Resources, University of California, Davis, CA 95616, USA*

(Received 24 September 1991; revision accepted 24 March 1992)

ABSTRACT

Luo, Y., Loomis, R.S. and Hsiao, T.C., 1992. Simulation of soil temperature in crops. Agric. For. Meteorol., 61: 23–38.

This paper presents a model that simulates soil temperature realistically with variable crop cover and soil water content and is also sufficiently small and fast to be included in a crop simulator. The model is developed according to principles of energy balance and soil heat transfer. Net radiation, sensible, latent, and ground-conductive heat fluxes are modified by foliage cover and cumulative evaporation as a basis for calculating the energy balance at the soil surface. Soil temperature at various depths is estimated with Fourier's heat transfer equation. One experiment measuring relative humidity at the soil surface was conducted to develop an equation for predicting vapor pressure at the soil surface. Two other field experiments measuring air and soil temperatures and energy balance components were carried out for model validation. The model well predicts energy fluxes at the soil surface, soil surface temperature, and soil temperature at various depths in crops. Canopy cover and soil surface wetness strongly influence energy balance and soil temperature whereas variation in soil porosity and soil thermal conductivity have little effect on soil temperature.

INTRODUCTION

Simulation of soil temperature facilitates study of root dynamics, activity of soil microbes, and nutrient availability. Three tyes of soil temperature models have been developed. The simplest, purely empirical, models are based on statistical relationships between soil temperature at some depth and climatological and soil variables (Toy et al., 1978; Cruse et al., 1980). These models are easy to construct and use, but require large data bases from which to develop empirical coefficients for each specific site. Mixed empirical and mechanistic models predict soil temperature with depth based on physical principles of heat flow (Wierenga and De Wit, 1970; Gupta et al., 1981), but the upper boundary temperature must be given or estimated empirically.

Correspondence to: R.S. Loomis, Agronomy and Range Science, University of California, Davis, CA 90024, USA.

A third type of model centers on physical processes (radiative energy balance and sensible, latent, and ground-conductive heat fluxes) to predict the upper boundary temperature. However, most existing process-oriented models simulate only simple systems. Van Bavel and Hillel (1976) and Stathers et al. (1985), for example, dealt with bare ground. Bristow et al. (1986) considered a surface with uniform residue cover whereas Ross et al. (1985) and Liakatas et al. (1986) modeled mulched surfaces. Horton et al. (1984) simulated surface temperature in a row crop with incomplete cover from the track of sun flecks. Calculations of sensible and latent heat fluxes, however, were not modified from the bare ground case.

Estimation of sensible and latent heat fluxes at a soil surface under vegetation cover is made difficult by temporal and spatial heterogeneities of the canopy, variable wetness of the soil surface, and wind gusts. Attempts to measure or to predict wind profiles and then eddy transport within canopies have been made (Monteith and Unsworth, 1990). Effects of canopy structure, wetness of the soil surface, and the wind vector on within-canopy transport, however, have not been quantified well (Ham and Heilman, 1991). Prediction of wetness at the soil surface meets even greater challenges owing to difficulties in measurement of soil-surface water status. Although volumetric soil water content in the surface layer and soil surface albedo can be measured (Idso et al., 1974, 1975), variation of water vapor pressure at the soil surface with canopy cover, atmospheric conditions, and soil water content are not fully understood. A stratified canopy model integrating air temperature, humidity, and wind velocity as well as radiation and (CO_2), for example, was undermined by sudden gusts of wind (Goudriaan, 1989).

Our objective here is to develop a process-oriented soil-temperature model that not only accounts for much of the complexity in crop fields but also is sufficiently simple for use in general crop models. The model named SLTMP is based on principles of energy balance and heat conduction in soil. The energy balance at the soil surface under vegetation cover is calculated after its components, net radiation, sensible, latent, and ground-conductive heat fluxes, are modified by foliage canopy and cumulative evaporation. The energy balance equation is solved by Newton's iterative numerical method to achieve a simultaneous estimate of soil-surface temperature for 1 h steps, providing the upper boundary condition for Fourier's heat-transfer equation. Soil temperature with depth was estimated with Fourier's equation.

THEORY

Energy fluxes and temperature at the soil surface

Soil surface temperature (T_0, °C) results from the energy balance (W m^{-2}) of net radiation (R_n) and latent (λE), sensible (H), and ground-conductive

(G) heat fluxes at the soil surface. Thus, temperature function at the surface $f(T_0)$ is

$$f(T_0) \quad = \quad R_n + \lambda E + H + G \tag{1}$$

This equation can be expanded as

$$\begin{aligned} f(T_0) \quad = \quad & R_l - \varepsilon_0 \sigma (T_0 + 237.2)^4 - \frac{C_a}{r_0}(T_0 - T_a) \\ & - \frac{0.622 \rho \lambda}{r_0 P}(e_0 - e_a) - \kappa \frac{T_0 - T_z}{z} \end{aligned} \tag{2}$$

where R_a is radiation absorbed at the soil surface (W m^{-2}) ε_0 is soil surface emissivity, σ is the Stefan-Boltzmann constant (5.67×10^{-8} W m^{-2} K^{-4}). C_a is volumetric heat capacity of air (J m^{-3} K^{-1}), r_0 is soil surface resistance (s m^{-1}), T_a is air temperature, ρ is air density (kg m^{-3}). P is atmospheric pressure (Pa), λ is the latent heat for water vaporization (J kg^{-1}), e_0 is water vapor pressure at the surface (Pa), e_a is air vapor pressure (Pa), κ is soil thermal conductivity (W m^{-1} K^{-1}), z is depth (m), and T_z is soil temperature at depth z.

R_a at the soil surface is estimated by

$$R_a \quad = \quad (1 - a)(R_b + R_d) + R_{l\downarrow} \tag{3}$$

where R_b and R_d are the incoming direct-beam and diffuse short-wave radiation fluxes, a is soil surface albedo, and $R_{l\downarrow}$ is the incoming long-wave radiation. R_b and R_d under vegetation are estimated with the Duncan stratified-canopy model (Duncan et al., 1967; Denison and Loomis, 1989). Albedo is estimated from soil volumetric water content in the first layer following Van Bavel and Hillel (1976). Incident long-wave radiation underneath the canopy comes from both sky and canopy. Using air temperature (T_a) as the first approximation of canopy temperature, then

$$R_{l\downarrow} \quad = \quad [\varepsilon_{ac}(1 - C_g) + \varepsilon_c C_g]\, \sigma\, (T_a + 273.2)^4 \tag{4}$$

where ε_{ac} is atmospheric emissivity estimated from air temperature and cloudiness (Campbell, 1977), ε_c is canopy emissivity (0.95), and C_g is fractional ground cover.

Soil surface resistance (r_0), introduced by Monteith (1981) and used by Lascano et al. (1987), was estimated with

$$r_0 \quad = \quad r_a e^{\alpha L} \tag{5}$$

where α is a parameter, / is leaf area index, and r_a is canopy resistance as

$$r_a \quad = \quad \frac{1}{\mathrm{k}^2 u_z}\left[\ln\left(\frac{z - d}{z_0}\right)\right]^2 \tag{6}$$

In this, k is von Karman's constant (0.40), u_z is wind speed (m s^{-1}) at height z (m), d is zero plane displacement (m), and z_0 is roughness length (m).

Air vapor pressure, e_a, is estimated from the wet bulb and dry bulb temperature with a psychrometric equation (Jones, 1983). Estimation of e_0 at a partially wet surface was suggested by Van Bavel and Hillel (1976) as

$$e_o = h_0 e^*(T_0) \tag{7}$$

where h_0 is relative humidity at the surface and $e^*(T_0)$ is saturation vapor pressure at T_0. Relative humidity at the soil surface was estimated with

$$h_0 = \bar{h} + A \sin\left(\frac{2\pi t}{24}\right) \tag{8}$$

where $\bar{h}$ and A are the daily average and amplitude of relative humidity, respectively, and are related to cumulative evaporation within a drying cycle (ΣE) as follows

$$\bar{h} = e^{(-\mathrm{k}_1 \Sigma E)} \tag{9}$$

and

$$A = \mathrm{k}_2 e^{(-\mathrm{k}_3/\Sigma E)} \tag{10}$$

where k_1, k_2, and k_3 are constants derived from measured data.

Equation 2 is solved with Newton's iterative technique (Bristow, 1987) as

$$T_{0,i+1} = T_{0,i} - \frac{f(T_{0,i})}{f'(T_{0,i})} \tag{11}$$

where $T_{0,i}$ and $T_{0,i+1}$ are the ith and $(i + 1)$ the approximate solutions of Eqn. 2, $f(T_{0,i})$ is the function $f(T_0)$ evaluated at $T_{0,i}$, and $f'(T_{0,i})$ is the first derivative of function $f(T_0)$ evaluated at $T_{0,i}$. Once $T_{0,i+1}$ is calculated, the process is repeated using $T_{0,i} = T_{0,i+1}$ until the difference between $T_{0,i+1}$ and $T_{0,i}$ is sufficiently small. The obtained soil surface temperature is used as the upper boundary condition for heat conduction in soil.

Heat conduction in soil

Change rate in heat content of a volume element of soil is equal to the change of heat flux with distance

$$C_s \frac{\partial T}{\partial t} = \frac{\partial \kappa \frac{\partial T}{\partial z}}{\partial z} \tag{12}$$

where C_s is volumetric heat capacity of soil ($\mathrm{J\,m^{-3}\,K^{-1}}$) and t is time. Using D_i for soil thermal diffusivity (κ/C_s, $\mathrm{m^2\,s^{-1}}$) between the midpoints of $(i-1)$th and ith layers, and z_i as depth of the midpoint, the equation is expanded numerically as

$$\frac{T_i^j - T_i^{j-1}}{t} = \frac{D_{i+1}\dfrac{T_{i+1} - T_i}{z_{i+1} - z_i} - D_i\dfrac{T_i - T_{i-1}}{z_i - z_{i-1}}}{\dfrac{z_{i+1} - z_{i-1}}{2}} \tag{13}$$

where T_i^j is the soil temperature at the midpoint of the ith layer in the jth (present) time step, T_i^{j-1} is soil temperature in the same layer but one time step in the past, and T_i is temperature in the ith layer at some time between the two time steps. In this model, time step is 1 h and the temperature 1 h in the past is used as T_i for simplicity. Thickness of the surface soil layers is 0.1 m to obtain a stable numerical solution (Simonson, 1975).

MATERIALS AND METHODS

Field experiments

Three experiments (labeled A, B, and C) were conducted in fields for measuring relative humidity at the soil surface, soil surface energy fluxes, and soil temperature. In Experiment A, a soil surface psychrometer (Seymour and Hsiao, 1984) was used to measure relative humidity at the surface at six sites in the middle of a large field of seedling maize on the University's experimental farm from 10 to 14 June 1989, following a furrow irrigation on 9 June. Maize was seeded in rows 0.76 m apart on a Yolo silt loam (fine-silty, mixed, thermic, Typic Zerochrepts, Inceptisol; Andrews, 1972). Ground cover, estimated from photographs taken from a verticle view, increased from 0.033 to 0.135 during the measurement period. Although accounted for in ALFALFA, cover was not an important factor in the experiment. The sites were about 10 m apart. At each site, four measurements were taken: top of beds, east slope, west slope, and furrow bottom. A Bowen-ratio apparatus (Held et al., 1990) was used to measure latent heat flux from which soil evaporation was derived using the approach by Hernandez-Suarez (1988).

In Experiment B, components of the energy balance (R_n, H, λE, and G) were measured with a Bowen-ratio apparatus (Held et al., 1990) in the middle of an alfalfa field on the University farm from 28 to 30 September 1991, after a forage harvest on 27 September. Two sets of wet- and dry-bulb platinum resistance thermometers were set 100 and 200 cm above the ground to measure T_a and e_a. H and λE were estimated with the Bowen-ratio method (Held et al., 1990).

In Experiment C, soil temperature at depths of 0, 15, 35, 100 cm (respectively 4, 4, 4, and 2 replicates) and air temperature at 1.5 m height (2 replicates) were measured in a fairly uniform alfalfa crop on the University farm from 6 May to 7 July 1987; 0.511 mm diameter (24-gauge) thermocouples and a data logger (CR5 Digital Recorder, Campbell Scientific, Logan, UT) were used. Thermocouples at the nominal depth of 0 cm were covered with a very thin layer of fine soil. All aerial thermocouples were protected by white shields. Temperatures were recorded every 2 h. No rain occurred during the experiment; the field was irrigated on 5 May, 4 June, and 17 June. When measurements began, the canopy was closed. The crop was cut on 29 May and 2 July at about 7 cm height.

Simulations

SLTMP was linked to the crop model ALFALFA (Denison and Loomis, 1989) which provided hourly values of R_b, R_d, θ, and L as input to SLTMP.

A series of simulations was conducted using parameters for a silt loam soil to demonstrate SLTMP behavior. In all simulations, soil water contents at field capacity and permanent wilting point were 0.27 (v/v) and 0.10 (v/v), respectively. Total soil porosity was 0.50 (v/v) and thermal conductivities for the silt loam soil were from Campbell (1985). Thicknesses of the ten soil layers were 10, 10, 30, 30, 40, 30, 30, 30, 30, and 60 cm from the surface to the depth of 3 m. Some of the thicknesses were chosen to match depths at which soil temperatures were measured in 1987. Initial soil temperature was the daily average of T_a for the starting day.

The model was run with weather data from the nearby UC Davis weather station in 1991 to predict energy fluxes at the soil surface for Experiment B. The simulation began on 15 August and ended on 2 October. Irrigation with 50 mm water was on 22 August and forage harvest at height of 7 cm was on 27 September.

The model also ran with Davis weather data for 1987 to predict T_0 and T_z. The simulation started on 19 April with a simulated leaf area index reaching about two on 6 May, similar to that observed in Experiment C. Irrigations with 100 mm water on 5 May, 4 June, and 17 June, and forage harvests on 29 May and 2 July at 7 cm height also matched those of Experiment C. The simulation ended on 3 July. Within the simulation period, two days, 9 May and 2 June, were simulated in detail as typical in foliage canopy cover and soil water content. On 9 May, 4 days after irrigation, the soil surface was wet and the leaf canopy was well developed. On 2 June, 4 days after cutting, the ground was nearly bare and the surface was dry.

RESULTS AND DISCUSSION

Relative humidity at the soil surface

Relative humidity at the soil surface (H_0) diurnally fluctuated with the daily amplitude becoming larger with time after irrigation (Fig. 1). H_0 peaked in the

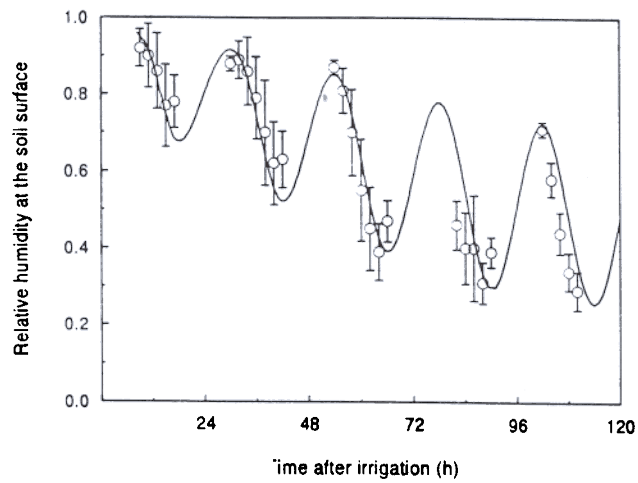

Fig. 1. Relative humidity at the soil surface on the University of California, Davis experimental farm from 10 to 14 June 1989. Data from Experiment A are presented as means $\pm$SD ($n = 24$). Line represents prediction with $H_0 = e^{\;0.037\Sigma E} + 0.30\,e^{-6.01/\Sigma E}\sin(2\pi t/24)$.

early morning and declined to a minimum in the late afternoon. Variation of H_0 measured at the 24 positions in Experiment A was small in the early morning, became larger in the middle of the day, and was small again in the late afternoon. Fitting Eqns. 8–10 to measured H_0 provided parameter values of 0.037, 0.30, and 6.01 for k_1, k_2, and k_3, respectively. Similar patterns of volumetric soil water content in the surface 0.25 cm layer were reported by Idso et al. (1975). Soil water content was high at 06 : 00 h and declined to the lowest value at 17 : 00 h, and diurnal amplitude increased with time after irrigation. Idso et al. (1974, 1975) used soil surface albedo to indicate surface wetness. In the second stage of evaporation, albedo was low in the early morning and increased until late afternoon.

Model validation

SLTMP reasonably predicted energy fluxes at the dry soil surface under small canopy cover on 28 September 1991 (Experiment B, Fig. 2). R_n was underestimated by about 20 W m^{-2} at noon. Sensible heat flux was overestimated (more negative) in the morning when latent heat flux was underestimated (less negative). Predicted ground-conductive heat flux well matched the field data. The soil was dry on 28 September 1991 and a significant portion of R_n was expended in heating the soil (Fig. 2).

The model predicted soil surface temperature well under contrasting conditions found in Experiment C (Figs. 3 and 4). Soil surface temperature (T_0) was close to air temperature (T_a) at night and became lower than T_a during

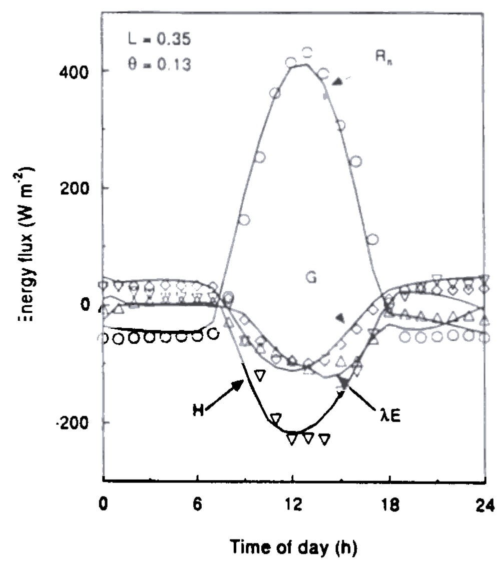

Fig. 2. Validation of energy balance at a dry and nearly bare soil surface at Davis, 28 September 1991, for Experiment B. Lines are model prediction, symbol (○) represents measured values R_n; (Δ) λE; (▽) H; (◇) G.

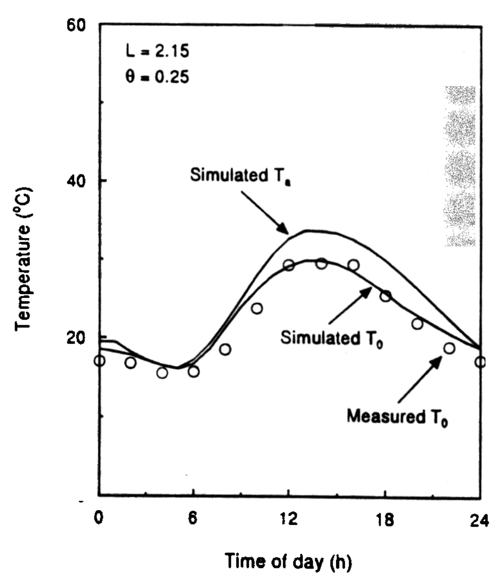

Fig. 3. Validation of soil surface temperature at a wet surface under a closed cover at Davis, 9 May 1987. Lines are simulated T_a and T_0. Symbol (○) is T_0 measured in Experiment C.

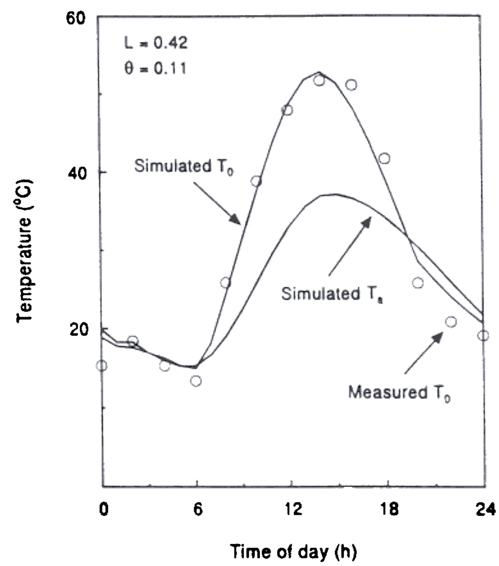

Fig. 4. Validation of soil surface temperature at a dry and nearly bare surface at Davis, 2 June 1987. Lines are simulated T_a and T_0. Symbol (O) is T_0 measured in Experiment C.

the daytime of 9 May 1987 when the soil surface was wet and the foliage canopy was well developed (Fig. 3). At noon, T_0 was nearly 4°C below T_a. On 2 June when the ground was nearly bare and the soil surface was dry, T_0 was about 14°C higher than T_a at noon whereas it was about 2°C cooler after 18:00 h (Fig. 4).

Soil temperature (T_z) fluctuated much less in deep soil layers than in the surface soil layer (Figs. 5 and 6). The amplitude at 35 cm was near zero and temperature at 100 cm was virtually constant during the entire day. T_z fluctuated more in a dry soil under a sparse canopy than in a wet soil under dense canopy cover (Fig. 5 vs. Fig. 6).

SLTMP predicts dynamics of T_z along the soil profile reasonably well in both the dry and wet soils (Figs. 5 and 6). Predicted daily maximum temperature at 15 cm was displaced about 2 h for both days. The displacement is probably owing to the use of temperature 1 h in the past in prediction of current temperature causing the model to overshoot the new temperature (Campbell, 1985).

Sensitivity analysis of the model

Effects of foliage cover and soil water content on energy fluxes and soil temperature in crops were investigated in simulations with four contrasting

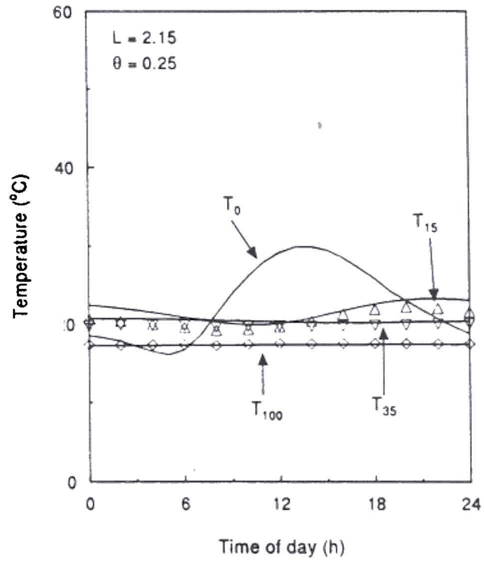

Fig. 5. Validation of soil temperature in a wet soil under a closed canopy at Davis, 9 May 1987, with data from Experiment C. Lines are simulated T_0 at the surface, T_{15} at 15 cm, T_{35} at 35 cm, and T_{100} at 100 cm depth. Symbol (△) represents measured soil temperature at 15 cm; (▽) at 35 cm; (◇) at 100 cm.

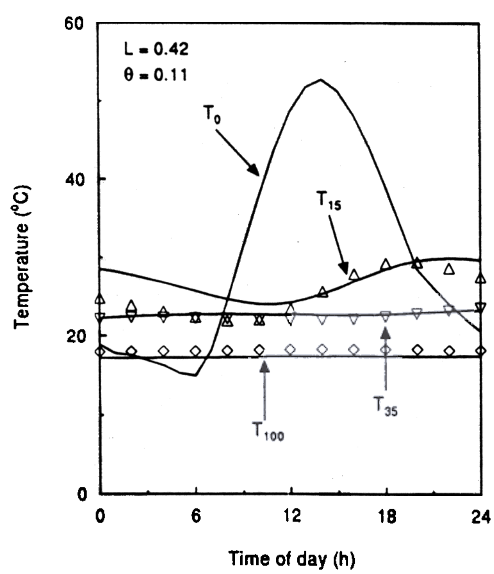

Fig. 6. Validation of soil temperature in a dry soil under small cover at Davis, 2 June 1987. Lines are simulated T_0 at the surface, T_{15} at 15 cm, T_{35} at 35 cm, T_{100} at 100 cm deep in soil. Symbol (△) represents soil temperature measured in Experiment C at 15 cm; (▽) at 35 cm; (◇) at 100 cm.

combinations of high or low canopy cover and high or low soil water content on 2 June 1987. Both canopy cover and soil water content strongly influenced energy fluxes at the soil surface (Fig. 7). When the canopy cover was low and the surface dry, R_n was large and was balanced mainly by sensible heat flux to air (H; Fig. 7(a)). When the canopy cover was small and the surface was wet, R_n was larger than with a dry surface (Fig. 7(b) vs. 7(a)) owing to less long-wave radiation loss. At the wet surface, most R_n was expended as latent heat for evaporation while sensible heat fluxes both to air (H) and to soil (G) were small (Fig. 7(b)). When the canopy cover was closed and the soil surface dry, R_n was very small and λE and H were nearly zero (Fig. 7(c)). R_n was dissipated mainly in G. At the wet soil surface under canopy cover, R_n was small and H was from air to the soil surface during most of the day and contributed additional energy to soil evaporation (Fig. 7(d)).

Energy fluxes predicted with the model were consistent with those measured in fields. Tanner (1960) measured energy balance components over alfalfa with different soil surface wetness and canopy covers. In a well irrigated alfalfa field with good cover, sensible heat from air contributed to latent heat flux in addition to net radiation. Fritschen and Van Bavel (1962) measured energy fluxes at moist and dry soil surfaces and concluded that when the soil was moist almost all of the energy supplied by net radiation was consumed as latent heat. By the Day 5 after irrigation, net radiation was almost equally partitioned among λE, H, and G.

Soil surface temperature varied with canopy cover and soil water content (Fig. 8). At the dry and nearly bare soil surface, T_0 ranged from 15.0 to 52.8°C (Fig. 8(a)) in comparison with the T_a range from 15.2 to 37.1°C. At the wet and nearly bare ground, the daily maximum of T_0 was 2°C higher than T_a (Fig. 8(b)). At the dry soil surface with a closed canopy, T_0 was close to T_a (Fig. 8(c)). At the wet soil surface under canopy cover, T_0 during the daytime was less than T_a (Fig. 8(d)). At noon, T_0 was about 8°C cooler than T_a. Soil water content also affected heat transfer in the soil. Temperature fluctuation at 15 cm was stronger in the wet soil than in the dry soil although T_0 at the dry soil was about 12°C higher than at the wet soil (Fig. 8(a) vs. 8(b)).

The daily pattern of the model's prediction of soil surface temperature under different conditions of canopy cover and soil water status is supported with measurements made by Gupta et al. (1981). With a bare soil surface, for example, they found that maximum daily surface temperature was 15°C higher than maximum daily air temperature. By contrast, maximum daily soil surface temperture was over 5°C lower in a maize crop and over 8°C lower in maize crop with residue than maximum daily air temperature. In addition, they found that daily minimum soil surface temperature did not differ by more than 2°C from daily minimum air temperature.

Sensitivity analyses on parameters for soil porosity and soil thermal conductivity were performed with four simulations. One of the parameters was

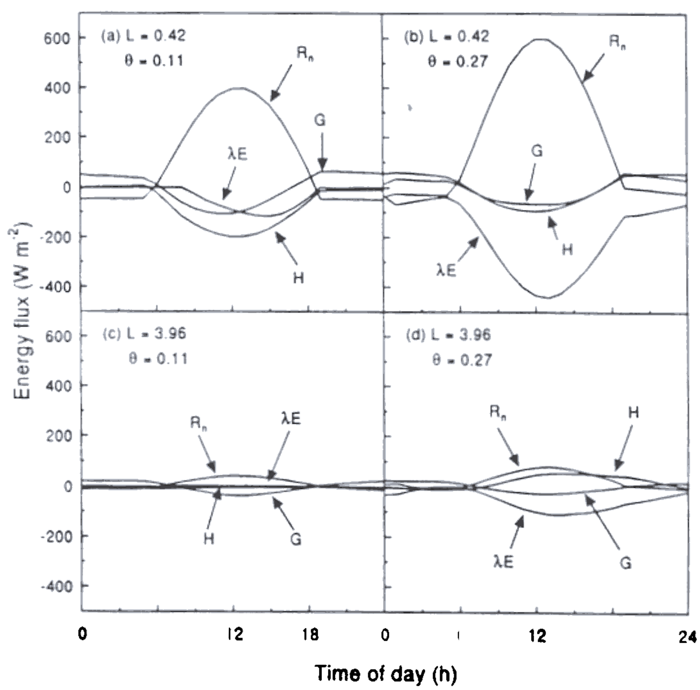

Fig. 7. Effects of canopy cover and soil water status on energy fluxes at the soil surface at Davis, 2 June 1987. (a) Low canopy cover and dry soil; (b) low canopy cover and wet soil; (c) high canopy cover and dry soil; (d) high canopy cover and wet soil.

either increased or decreased by 20% in each simulation (Table 1). Changes in soil porosity and conductivity had little effect on T_0 but caused some differences in T_z in deep layers because they affected heat transfer while having little effect on the energy balance at the surface. Similar results were reported by Stathers et al. (1985) that soil temperature was not sensitive to changes of soil thermal parameters.

In summary, SLTMP, a process-oriented model that integrates canopy cover and soil water status in addition to dominant weather factors and soil properties into a soil temperature simulator, predicts energy fluxes at the soil surface, surface temperature (T_0), and temperature (T_z) with depth quite well. On dry and nearly bare ground, most R_n was dissipated as sensible heat, $T_0 \gg T_a$ during the day and $T_0 < T_a$ at night, and soil temperature fluctuation was damped quickly with depth. With the wet soil and little canopy cover, most R_n was converted to latent heat and T_0 is only a few degrees higher than T_a during the day. Ground heat conducted to deeper soil layers. With a dry soil surface and canopy cover, little solar radiation reached the bottom of the canopy and evaporation was also small. T_0 was close to T_a. On wet soil

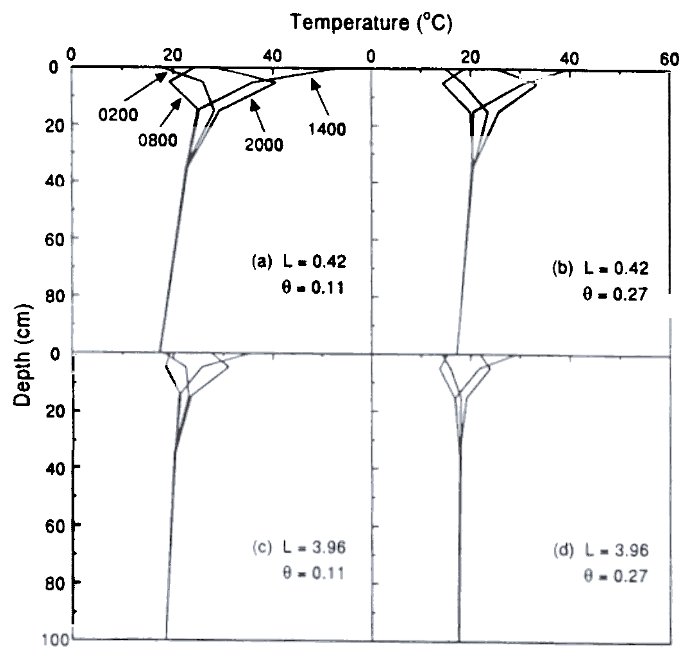

Fig. 8. Effects of canopy cover and soil water status on soil temperature along the profile in Yolo silt loam at Davis, 2 June 1987. (a) Low canopy cover and dry soil; (b) low canopy cover and wet soil; (c) high canopy cover and dry soil; (d) high canopy cover and wet soil.

TABLE

Simulated differences of daily maximum (MX) and minimum (MN) soil temperatures (°C) between control and treatments on 9 May and 2 June 1987. The control is the standard soil-temperature simulation. In the treatment simulations, either soil porosity or thermal conductivity was changed by ±20%

Date	Variable	Change	Depth (cm)					
			0		15		100	
			MN	MX	MN	MX	MN	MX
9 May	Porosity	−20%	0.1	−0.1	0.2	−0.3	−0.3	−0.3
9 May	Porosity	+20%	−0.1	0.1	−0.2	0.3	0.4	0.4
9 May	Conductivity	−20%	0.2	0.1	0.3	−0.5	−0.7	−0.7
9 May	Conductivity	+20%	0.0	−0.1	−0.3	0.4	0.6	0.5
2 June	Porosity	−20%	0.3	−0.2	0.3	−0.8	−0.2	−0.3
2 June	Porosity	+20%	−0.4	0.3	−0.5	1.1	0.3	0.3
2 June	Conductivity	−20%	−0.1	0.3	0.3	−1.3	−0.4	−0.5
2 June	Conductivity	+20%	0.0	−0.2	−0.4	1.2	0.4	0.5

with canopy cover, net radiation was small, latent heat flux took energy away from the surface, and sensible heat flux went from air to the surface and contributed additional energy for soil evaporation. T_0 during the day was less than T_a while at night it was close to or even higher than T_a. These sets of SLTMP in a series of warm-season studies give confidence that the model has considerable robustness for its intended use. Additional evaluations under cool and humid conditions would be useful.

REFERENCES

Andrews, W.F., 1972. Soil survey of Yolo county, California. Soil Conservation Service, USDA, Washington, DC.

Bristow, K.L., 1987. On solving the surface energy balance equation for surface temperature. Agric. For. Meteorol., 39: 49–54.

Bristow, K.L., Campbell, G.S., Papendick, R.I. and Elliott, L.F., 1986. Simulation of heat and moisture transfer through a surface residue-soil system. Agric. For. Meteorol., 36: 193–214.

Campbell, G.S., 1977. An introduction to environmental biophysics. Springer-Verlag, New York, 159 pp.

Campbell, G.S., 1985. Soil physics with BASIC: Transport models for soil-plant systems. Elsevier, Amsterdam, 150 pp.

Cruse, R.M., Linden, D.R., Radke, J.K. and Larson, W.E., 1980. A model to predict tillage effect on soil temperature. Soil Sci. Soc. Am. J., 44: 378–383.

Denison, R.F. and Loomis, R.S., 1989. An integrative physiological model of alfalfa growth and development. Div. Agric. Nat. Res. Publ. No. 1926. University of California, Oakland, 73 pp.

Duncan, W.G., Loomis, R.S., Williams, W.A. and Hanau, R., 1967. A model for simulating photosynthesis in plant communities. Hilgardia, 38: 181–205.

Fritschen, L.J. and van Bavel, C.H.M., 1962. Energy balance components of evaporating surfaces in arid lands. J. Geophys. Res. 67: 5179–5185.

Goudriaan, J., 1989. Simulation of micrometeorology of crops, some methods and their problems, and a few results. Agric. For. Meteorol., 47: 239–258.

Gupta, S.C., Radke, J.K. and Larson, W.E., 1981. Predicting temperatures of bare and residue covered soils with and without a corn crop. Soil Sci. Soc. Am. J., 45: 405–412.

Ham, J.M. and Heilman, J.L., 1991. Aerodynamic and surface resistances affecting energy transport in a sparse crop. Agric. For. Meteorol., 53: 267–284.

Held, A.A., Steduto, P., Orgaz, F., Matista, A. and Hsiao, T.C., 1990. Bowen ratio/energy balance technique for estimating crop net CO_2 assimilation, and comparison with a canopy chamber. Theor. Appl. Climat., 42: 203–213.

Hernandez-Suarez, M., 1988. Modeling irrigation scheduling and its components, and optimization of water delivery schedules with dynamic programming and stochastic ET_0 data. Ph.D. dissertation. University of California, Davis, CA.

Horton R., Aguirre-Luna, O. and Wierenga, P.J., 1984. Soil temperature in a row crop with incomplete surface cover. Soil Sci. Soc. Am. J., 48: 1225–1232.

Idso, S.B., Aase, J.K., Jackson, R.D., 1975. Net radiation — soil heat flux relations as influenced by soil water content variations. Boundary-Layer Meteorol., 9: 113–122.

Idso, S.B., Reginato, R.J., Jackson, R.D., Kimball, B.A. and Nakayama, F.S., 1974. The three stages of drying of a field soil. Soil Sci. Soc. Am. J., 38: 831–837.

Jones, H.G., 1983. Plants and microclimate: A quantitative approach to environmental plant physiology. Cambridge University Press, Cambridge, 323 pp.

Lascano, R.J., van Bavel, C.H.M., Hatfield, J.L. and Upchurch, D.R., 1987. Energy and water balance of a sparse crop: Simulated and measured soil and crop evaporation. Soil Sci. Soc. Am. J., 51: 1113-1121.

Liakats, A., Clarke, J.A. and Monteith, J.L., 1986. Measurements of the heat balance under plastic mulches. Part I. Radiation balance and soil heat flux. Agric. For. Meteorol., 36: 227-239.

Monteith, J.L. 1981. Evaporation and surface temperature. Q. J. R. Meteorol. Soc., 107: 1-27.

Monteith, J.L. and Unsworth, M.H., 1990. Principles of environmental physics. 2nd edn. Edward Arnold, London, 291 pp.

Ross, P.J., Williams, J. and McCowen, R.L., 1985. Soil temperature and the energy balance of vegetative mulch in the semi-arid tropics. II. Dynamic analysis of the total energy balance. Aust. J. Soil. Res., 23: 515-532.

Seymour, V.A. and Hsiao, T.C., 1984. A soil surface psychrometer for measuring humidity and studying evaporation. Agric. For. Meteorol., 32: 61-70.

Simonson, J.R., 1975. Engineering heat transfer. Macmillan, London.

Strathers, R.J., Black, T.A. and Novak, M.D., 1985. Modelling soil temperature in forest clearcuts using climate station data. Agric. For. Meteorol., 36: 153-164.

Tanner, C.B. 1960. Energy balance approach to evapotranspiration from crops. Soil Sci. Soc. Am. Proc., 24: 1-9.

Toy, T.J., Kuhaida, A.J., Jr., and Munson, B.E., 1978. The prediction of mean monthly soil temperature from mean monthly air temperature. Soil Sci., 126: 96-104.

Van Bavel, C.H.M. and Hillel, D.I., 1976. Calculating potential and actual evaporation from a bare soil surface by simulation of concurrent flow of water and heat. Agric. Meteorol., 17: 453-476.

Wierenga, P.J. and de Wit, C.T., 1970. Simulation of heat flow in soils. Soil Sci. Soc. Am. Proc., 34: 845-848.

APPENDIX

Symbol	Meaning	Unit
a	Albedo	
d	Zero plane displacement	m
e_a	Air vapor pressure	Pa
e_0	Vapor pressure at the soil surface	Pa
e^*	Saturation vapor pressure	Pa
h_0	Relative humidity at the soil surface	
k	von Karman constant	-
r_0	Soil surface resistance	$\mathrm{s\,m^{-}}$
r_a	Boundary layer resistance of canopy	$\mathrm{s\,m^{-}}$
u_z	Wind speed at height z	$\mathrm{m\,s^{-}}$
z	Depth or height	m
z_0	Roughness length	m
A	Diurnal amplitude of relative humidity at the soil surface	
C_a	Volumetric heat capacity of air	$\mathrm{J\,m^{-3}\,K^{-1}}$
C_g	Canopy cover	-
C_s	Volumetric heat capacity of soil	$\mathrm{J\,m^{-3}\,K^{-1}}$
D	Soil thermal diffusivity	$\mathrm{m^2\,s^{-1}}$
E	Evaporation	$\mathrm{kg\,m^{-2}\,s^{-1}}$

λE	Latent heat flux	$W\,m^{-2}$
G	Ground-conductive heat flux	$W\,m^{-2}$
H	Sensible heat flux	$W\,m^{-2}$
L	Leaf area index	$m^2\,m^{-2}$
P	Atmospheric pressure	Pa
R_a	Absorbed radiation at the soil surface	$W\,m^{-2}$
R_b	Direct-beam short-wave radiation	$W\,m^{-2}$
R_d	Diffuse short-wave radiation	$W\,m^{-2}$
$R_{l\downarrow}$	Long-wave radiation incident to the soil	$W\,m^{-2}$
R_n	Net radiation at the soil surface	$W\,m^{-2}$
T_0	Soil surface temperature	°C
T_a	Air temperature	°C
T_z	Soil temperature at depth z	°C
ε_0	Emissivity at the soil surface	
ε_{ac}	Atmospheric emissivity	
ε_c	Canopy emissivity	
θ	Volumetric soil water content	$m^3\,m^{-3}$
κ	Thermal conductivity of soil	$W\,m^{-1}\,K^{-1}$
λ	Latent heat of water vaporization	$J\,Kg^{-1}$
ρ	Air density	$Kg\,m^{-3}$
σ	Stefan–Boltzmann constant	$W\,m^{-2}\,K^{-4}$

λE	Latent heat flux	$W\,m^{-2}$
G	Ground-conductive heat flux	$W\,m^{-2}$
H	Sensible heat flux	$W\,m^{-2}$
L	Leaf area index	$m^2\,m^{-2}$
P	Atmospheric pressure	Pa
R_a	Absorbed radiation at the soil surface	$W\,m^{-2}$
R_b	Direct-beam short-wave radiation	$W\,m^{-2}$
R_d	Diffuse short-wave radiation	$W\,m^{-2}$
$R_{l\downarrow}$	Long-wave radiation incident to the soil	$W\,m^{-2}$
R_n	Net radiation at the soil surface	$W\,m^{-2}$
T_0	Soil surface temperature	°C
T_a	Air temperature	°C
T_z	Soil temperature at depth z	°C
ε_0	Emissivity at the soil surface	
ε_{ac}	Atmospheric emissivity	
ε_c	Canopy emissivity	
θ	Volumetric soil water content	$m^3\,m^{-3}$
κ	Thermal conductivity of soil	$W\,m^{-1}\,K^{-1}$
λ	Latent heat of water vaporization	$J\,Kg^{-1}$
ρ	Air density	$Kg\,m^{-3}$
σ	Stefan–Boltzmann constant	$W\,m^{-2}\,K^{-4}$